

Theoretical study on ThF⁺, a prospective system in search of time-reversal violation

Denis, Malika; Norby, Morten S.; Jensen, Hans Jorgen Aa; Gomes, André Severo Pereira; Nayak, Malaya K.; Knecht, Stefan; Fleig, Timo

Published in:
New Journal of Physics

DOI:
10.1088/1367-2630/17/4/043005

Publication date:
2015

Document version:
Final published version

Document license:
CC BY

Citation for pulished version (APA):
Denis, M., Norby, M. S., Jensen, H. J. A., Gomes, A. S. P., Nayak, M. K., Knecht, S., & Fleig, T. (2015). Theoretical study on ThF⁺, a prospective system in search of time-reversal violation. *New Journal of Physics*, 17, [043005]. <https://doi.org/10.1088/1367-2630/17/4/043005>

Go to publication entry in University of Southern Denmark's Research Portal

Terms of use

This work is brought to you by the University of Southern Denmark.
Unless otherwise specified it has been shared according to the terms for self-archiving.
If no other license is stated, these terms apply:

- You may download this work for personal use only.
- You may not further distribute the material or use it for any profit-making activity or commercial gain
- You may freely distribute the URL identifying this open access version

If you believe that this document breaches copyright please contact us providing details and we will investigate your claim.
Please direct all enquiries to puresupport@bib.sdu.dk



PAPER • OPEN ACCESS

Theoretical study on ThF^+ , a prospective system in search of time-reversal violation

To cite this article: Malika Denis *et al* 2015 *New J. Phys.* **17** 043005

View the [article online](#) for updates and enhancements.

Related content

- [Accurate calculations of the ground state and low-lying excited states of the \$\(\text{RbBa}\)^+\$ molecular ion: a proposed system for ultracold reactive collisions](#)
S Knecht, L K Sørensen, H J Aa Jensen *et al.*
- [Spectroscopic and electric properties of the LiCs molecule](#)
L K Sørensen, T Fleig and J Olsen
- [Many-body theory of the electric dipole moment of atomic ytterbium](#)
Angom Dilip, Bhanu Pratap Das, Warren F Perger *et al.*

Recent citations

- [P,T-odd and magnetic hyperfine-interaction constants and excited-state lifetime for \$\text{HF}^+\$](#)
Timo Fleig
- [Methods, analysis, and the treatment of systematic errors for the electron electric dipole moment search in thorium monoxide](#)
J Baron *et al*
- [In search of discrete symmetry violations beyond the standard model: Thorium monoxide reloaded](#)
Malika Denis and Timo Fleig



PAPER

Theoretical study on ThF^+ , a prospective system in search of time-reversal violation

OPEN ACCESS

RECEIVED

6 December 2014

REVISED

23 February 2015

ACCEPTED FOR PUBLICATION

2 March 2015

PUBLISHED

2 April 2015

Content from this work
may be used under the
terms of the [Creative
Commons Attribution 3.0
licence](#).

Any further distribution of
this work must maintain
attribution to the
author(s) and the title of
the work, journal citation
and DOI.

Malika Denis¹, Morten S Nørby², Hans Jørgen Aa Jensen², André Severo Pereira Gomes³, Malaya K Nayak^{1,4}, Stefan Knecht⁵ and Timo Fleig¹¹ Laboratoire de Chimie et Physique Quantiques, IRSAMC, Université Paul Sabatier Toulouse III, 118 Route de Narbonne, F-31062 Toulouse, France² University of Southern Denmark, Department of Physics, Chemistry and Pharmacy, Campusvej 55, DK-5230, Odense, Denmark³ Laboratoire de Physique des Lasers, Atomes et Molécules (PhLAM), CNRS UMR 8523, Université de Lille, Bât P5, F-59655 Villeneuve d'Ascq Cedex, France⁴ Bhabha Atomic Research Centre, Trombay, Mumbai-400085, India⁵ ETH Zürich, Laboratorium für Physikalische Chemie, Vladimir-Prelog-Weg 2, CH-8093 Zürich, SwitzerlandE-mail: stefan.knecht@phys.chem.ethz.ch and timo.fleig@irsamc-ups-tlse.fr**Keywords:** electron electric dipole moment, P , T symmetry violation, relativistic electronic structure, hyperfine interaction, electronically excited states, wavefunction theory**Abstract**

The low-lying electronic states of ThF^+ , a possible candidate in the search for \mathcal{P} - and \mathcal{T} -violation, have been studied using high-level correlated relativistic *ab initio* multi-reference coupled-cluster and configuration interaction approaches. For the $^3\Delta$ state component with $\Omega = 1$ (electron electric dipole moment ‘science state’) we obtain an effective electric field of $E_{\text{eff}} = 35.2 \text{ GV cm}^{-1}$, a \mathcal{P} - and \mathcal{T} -odd electron–nucleon interaction constant of $W_{P,T} = 48.4 \text{ kHz}$, a magnetic hyperfine interaction constant of $A_{\parallel} = 1833 \text{ MHz}$ for ^{229}Th ($I = 5/2$), and a very large molecular dipole moment of 4.03 D. The $\Omega = 1$ state is found to be more than 300 cm^{-1} lower in energy than $\Omega = 0^+$ ($^1\Sigma^+$), challenging the state assignment from an earlier theoretical study on this species (Barker *et al* 2012 *J. Chem. Phys.* **136** 104305).

1. Introduction

The enormous surplus of matter over antimatter in our Universe is a fact that remains unexplained by the standard model (SM) of elementary particles [1]. A microscopic violation of the combined symmetries charge (C) conjugation and spatial parity (\mathcal{P}) has been identified as one of several conditions [2] which can give rise to an appreciable baryon number and explain this asymmetry. It is expected that flavor-diagonal $C\mathcal{P}$ violation, absent in the SM, must be sought for [3] and that electric dipole moments (EDMs) [4] constitute a sensitive probe of such new physics beyond the SM. Given the validity of the $C\mathcal{PT}$ theorem [5], the measurement of an EDM would be the first direct signature of the violation of time-reversal (\mathcal{T}) invariance [6].

The electron’s EDM has, despite a vigorous search for over half a century, still not been detected. The most constraining upper bounds on the electron EDM have for some time been obtained from experimental and theoretical investigations on atoms [7, 8], and such upper bounds are useful guiding constraints on beyond SM theories [9]. However, polar diatomic molecules have become the major players in this quest, since they offer an orders of magnitude larger enhancement [7, 10] of the ensuing energy shift than what could be achieved with an atom [11, 12]. This means that, for a given measurement on a molecular system, the possible magnitude of the electron EDM is constrained to a smaller value, or conversely, that the effect of a smaller electron EDM can be detected through the measurement. The corresponding enhancement factor is not accessible by experimental means and has to be determined—preferably—via a molecular relativistic many-body calculation.

According to the most recent findings using the polar molecule ThO [13–16] the upper bound on the electron EDM is $|d_e| < 9.6 \times 10^{-29} e \text{ cm}$. This value is more than 16 times smaller than the most constraining upper bound from an atomic study [12]. Charged molecules offer an experimental advantage over neutral

systems in that ion traps can be used which allow for long interrogation times. High-resolution spectroscopy employing rotating electric fields has been presented recently as a viable technique for symmetry violation searches in charged molecular ions [17, 18]. The ionic systems used in these experiments are HfF^+ and, as a perspective molecular ion, ThF^+ .

What the afore-mentioned molecules, and several others such as HfH^+ , PtH^+ [19] and WC [20, 21], have in common is an energetically low-lying $^3\Delta$ electronic state (in Λ - S coupling picture). In the fluorides and oxides this state is deeply bound which is an experimental advantage. The magnetic moment in the $\Omega = 1$ component of this term is approximately zero which helps reduce the vulnerability of the experiment to decoherence and systematic errors [17].

HfF^+ and ThF^+ exhibit a considerably large EDM effective electric field in the relevant ‘science’ state [22–24] and, at the same time, a small Λ (or Ω) doublet splitting. This latter property is an asset for efficient mixing of rotational parity eigenstates through the external electric laboratory field. While HfF^+ has been characterized in detail [22, 23, 25–28] considerably less is known for ThF^+ [24, 29, 30]. The joint experimental and theoretical work of Barker *et al* [29] left some uncertainty as to whether the $\Omega = 1$ state is the ground-state or the first excited state, as there is an $\Omega = 0^+$ state ($^1\Sigma_0^+$) separated from it by only 315 cm^{-1} . The experimental resolution was not sufficient to unequivocally assign those states and, unlike HfF^+ , the $\Omega = 1$ and 0^+ states of ThF^+ possess similar vibrational frequencies at around 658 cm^{-1} . Accompanying theoretical calculations were also inconclusive, but from the best estimate the $\Omega = 0^+$ state was proposed as ground state with the $\Omega = 1$ state higher by 65 cm^{-1} in [29] and 202 cm^{-1} in [31], respectively.

Turning to the EDM effective electric field in $\Omega = 1$ of ThF^+ , the work of Meyer *et al* [24] suggests an extremely large value of $E_{\text{eff}} = 90 \text{ GV cm}^{-1}$. Recent and more rigorous relativistic many-body calculations on the isoelectronic ThO molecule have shown [14, 15] that the model calculation of Meyer *et al* yields a significantly overestimated E_{eff} for the case of ThO (by more than 35%). It can therefore be expected that for this kind of molecules and electronic states the model of Meyer *et al* contains a systematic error that is also present in the above prediction for E_{eff} in ThF^+ .

We pursue two major goals in this work. Using spinor-based many-body methods which treat dynamic electron correlations and electronic spin–orbit interactions on the same footing, a rigorous determination of the electronic ground state of ThF^+ and some of its low-lying electronically excited states is carried out. Second, with the same uncompromising techniques we determine with high accuracy properties of the $^3\Delta_1$ ($\Omega = 1$) state which are of direct relevance for proposed measurements of the electron EDM. In particular, we present the first rigorous calculation of the eEDM \mathcal{P} , \mathcal{T} -odd interaction constant and of the molecular static electric dipole moment. Furthermore, the magnetic hyperfine interaction constant is calculated for $\Omega = 1$ along with the scalar–pseudoscalar \mathcal{P} , \mathcal{T} -odd interaction constant, both of which play an important role in the interpretation of corresponding and ongoing experimental measurements [18, 32]. We also calculated static molecular EDMs and electric transition moments, the latter of which are of interest regarding state preparation in an EDM experiment. Molecular dipole moments are directly related to the EDM effective electric field, since they are a measure of the mixing of parity eigenstates.

The manuscript is structured as follows: section 2 summarizes underlying theory and gives a concise account of the employed electronic-structure methods. In section 3 we present results and their discussion, preceded by a brief summary of relevant technical details for the calculations that have been carried out. In the final section 4 we summarize the major findings and draw conclusions for future work.

2. Theory and methods

2.1. Theory

The potential energy due to the electron EDM interaction in the molecule is determined as an expectation value over the effective one-body Hamiltonian $\hat{H}_{\text{edm}}^{\text{eff}}$ in accord with stratagem II of Lindroth *et al* [33]

$$\left\langle \hat{H}_{\text{edm}}^{\text{eff}} \right\rangle_{\psi} = \frac{2icd_e}{e\hbar} \left\langle \sum_{j=1}^n \gamma_j^0 \gamma_j^5 \mathbf{p}_j^2 \right\rangle_{\psi}, \quad (1)$$

where n is the number of electrons, γ are the standard Dirac matrices, d_e is the electron electric dipole moment, and \mathbf{p}_j the momentum operator for electron j .

The parallel magnetic hyperfine interaction constant A_{\parallel} is defined as the z projection of the expectation value of the corresponding perturbative Hamiltonian in Dirac theory

$$A_{\parallel} = \frac{\mu_{\text{Th}}}{I\Omega} \left\langle \sum_{i=1}^n \left(\frac{\vec{\alpha}_i \times \vec{r}_i}{r_i^3} \right)_z \right\rangle_{\psi}, \quad (2)$$

where I is the nuclear spin quantum number, α_k is a Hamiltonian-form Dirac matrix for particle k , and n is the number of electrons. Details on the implementation of the two afore-mentioned operators can be found in references [14, 23].

The \mathcal{P} , \mathcal{T} -odd interaction constant $W_{P,T}$ arising from the electron–nucleon scalar–pseudoscalar (S–PS) interaction is determined as the expectation value over the \mathcal{P} , \mathcal{T} -odd Hamiltonian

$$W_{P,T} = \frac{1}{k_s \Omega} \langle H_s \rangle_{\psi}, \quad (3)$$

where k_s is the electron–nucleus S–PS coupling constant. The interaction Hamiltonian H_s is defined [34] as

$$H_s = i \frac{G_{\text{F}}}{\sqrt{2}} Z k_s \sum_{j=1}^n \gamma_j^0 \gamma_j^5 \rho_N(r_j), \quad (4)$$

where $\rho_N(r_j)$ is the nuclear charge density at position r_j normalized to unity, G_{F} is the Fermi constant and k_s is a dimensionless S–PS interaction constant. The latter is defined as $Zk_s = (Zk_{s,p} + Nk_{s,n})$, where $k_{s,p}$ and $k_{s,n}$ are electron–proton and electron–neutron coupling constants, respectively. Equations (2) and (3) are evaluated as expectation values over the CI wavefunction for the $\psi_{\Omega=1}$ state.

2.2. Methods

All approaches employed in the present work are spinor-based molecular many-body methods in the framework of the four-component *no-virtual-pair* approximation (see [35] and references therein). For the treatment of dynamic interelectronic correlations linear and nonlinear (exponential) expansions of the molecular wavefunctions have been employed. As to the latter, we applied the coupled cluster approach [36] in a modern implementation, the intermediate Hamiltonian Fock-space coupled cluster including single and double excitations (IHFSCC) [37–41]. The linear expansions have been carried out with the general-active-space configuration interaction (GASCI) method [42, 43], implemented as the KR-CI module [44] in the DIRAC12 [45] relativistic electronic-structure program package.

3. Application to ThF⁺

3.1. Technical details

Calculations of spectroscopic properties were performed with the DIRAC12 program [45], except for vertical excitation energies of the $\Omega = 1$ state using refined active spinor spaces, which were carried out with a modified local version of the DIRAC11 program package [46]. This latter program version was also used for determining all \mathcal{P} , \mathcal{T} -odd and magnetic hyperfine expectation values.

We employed uncontracted atomic Gaussian basis sets for the description of both atoms' electronic shells. For thorium, Dyall's [47, 48] double- ζ (DZ, dyall.cv2z, [26s23p17d13f1g]) triple- ζ (TZ, dyall.cv3z, [33s29p20d15f5g1h]) for IHFSCC and CI models I^{CI} and II^{CI} and TZ', [33s29p20d14f4g1h] for all other CI models), and quadruple- ζ (QZ, dyall.cv4z, [37s34p26d23f9g5h1i]) for IHFSCC and CI models I^{CI} and II^{CI} and QZ', [37s34p24d19f7g4h] for all other CI models) basis sets were used. For the latter basis set, QZ', all 5d, 6d, 7s correlating functions, except for the i function, have been added. For the fluorine atom, aug-cc-pVnZ ($n = T, Q$) and cc-pVnZ ($n = D, T, Q$) [49] basis sets have been used.

For all wavefunction models of type \mathcal{N}^{CC} , I^{CI} and II^{CI} (see next paragraph for model definitions) we used the exact two-component Hamiltonian scheme of Illiaš and Saue [50] where two-electron spin-same-orbit (SSO) and spin-other-orbit (SOO) corrections were either obtained by means of atomic mean-field integrals [51, 52] (amf) or in a molecular mean-field approach [53] (mmf), based on the X2C transformation of the converged four-component Fock operator. For the models III^{CI} and IV^{CI} molecular spinors were optimized through all-electron four-component Dirac–Coulomb Hartree–Fock calculations. We based the open-shell calculations on an average-of-configuration Fock operator for two electrons in the three Kramers pairs of Th(7s, 6d δ), the other 96 electrons are restricted to closed shells.

The IHFSCC calculations on ThF⁺ were performed via the (0h, 2p) sector of Fock-space, by taking as closed-shell reference the ThF³⁺ cation and following the route:

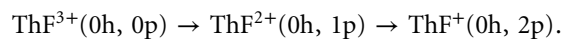


Table 1 summarizes the three different model ($P = P_m + P_i$) and correlating (Q) spaces which we explored in the IHFSCC singles and doubles calculations. The main model (P_m) space always comprised the virtual ThF³⁺

Table 1. Active (P_m, P_i) and correlation spaces (Q) in terms of thorium spinors (the F 2s, 2p spinors are always included in the occupied Q space). In case of MRCI the maximum excitation level for a given space is denoted as singles (S) and singles–doubles (SD), respectively.

Model	Th spinor distribution on spaces					
	4f5s5p	5d	6s6p	5f6d7s	7p7d8s8p6f	
IHFSCC	I^{CC}	frozen	frozen	Q	P_m	P_i
	II^{CC}	frozen	Q	Q	P_m	P_i
	III^{CC}	Q	Q	Q	P_m	P_i
MRCI	I^{CI}	frozen	$Q - S$	$Q - S$	P_m	$Q - SD$
	II^{CI}	frozen	$Q - SD$	$Q - SD$	P_m	$Q - SD$

spinors with Th 5f, 6d, 7s character while the Th 7p spinors were included in the intermediate space P_i . Spinors with Th 7d, 8s, 8p and 6f character were added to the P_i and all remaining virtuals were kept in the Q space. A total number of 462 (818) virtual spinors were considered in the correlation treatment using the TZ (QZ) basis set combinations which corresponds in each case to an energy cutoff in the virtual space of $\approx 95 E_H$. We have explored three different occupied Q spaces, all of which comprised the spinors with F 2s, 2p character. The first Q space contains in addition the spinors with Th 6s, 6p character, and corresponds to correlating 16 electrons (denoted in the following as I^{CC}); the second (II^{CC}) and third one (III^{CC}) includes the spinors with Th 6s, 6p, 5d and Th 6s, 6p, 5d, 4f, 5s, 5p character, respectively, correlating in total 26 (48) electrons.

The first motivation for choosing these active spaces is the attempt to obtain the highest possible accuracy while avoiding intruder states in the calculations. Accuracy in IHFSCC calculations is linked to both the dimension of the model space P (it has been argued [54] that large P spaces may alleviate the need of considering triple or higher excitations in the dynamical correlation treatment due to the inclusion of corresponding excited determinants in the effective Hamiltonian) as well as of the intermediate space P_m (states with their largest components in P_m are described more accurately than those for which the largest components are in P_i [41]). Secondly, considering a purely ionic model (Th^{2+}F^-), one may expect from the electronic structure of the Th^{2+} ion in particular states to arise from the 6d5f manifold [55], whereas in the covalent (Th^{1+}F) case electronic states arising from the 6d²7s manifold of atomic Th^+ will play an important role.

The MRCI expansions for the spectroscopic studies, summarized in the lower part of table 1, are based on an average-of-configuration Fock operator for two electrons in 12 spinors (Th 7s6d) restricting all other electrons to closed shells. We considered two active space choices, I^{CI} and II^{CI} , respectively, which differ by the maximum allowed excitation level of singles (S) and singles–doubles (SD) from the Th 5d6s6p + F 2s2p space into the model space P_m comprising the Th 5f, 6d, 7s spinors. Due to limited resources, the virtual space was restricted to spinors below an energy of $20 E_H$.

We defined models of varying quality to perform GASCI calculations of the effective electric field E_{eff} , the parallel magnetic hyperfine interaction constant A_{\parallel} , the scalar–pseudoscalar electron–nucleon interaction constant $W_{p,T}$ in the $\Omega = 1$ state and the vertical excitation energy T_v of the $\Omega = 0$ state.

We used two principal CI models, denoted as III^{CI} and IV^{CI} , the former of which has been further refined to accommodate for varying size of the valence spinor space and for the inclusion of determinants with more than two particles in the virtual spinor space. This elaborate choice of models is motivated by earlier findings on the ThO system [14]. The models are defined in full detail in table 2, using the nomenclature from table 1, for coherence.

For the calculation of the nuclear magnetic hyperfine coupling constant we use the thorium isotope ^{229}Th for which the nuclear magnetic moment has been determined to be $\mu = 0.45\mu_N$ [56]. Its nuclear spin quantum number is $I = 5/2$. In all calculations the speed of light was set to 137.0359998 a.u.

3.2. Results and discussion

3.2.1. Spectroscopic properties

In order to settle the question about which state is the ground state we have carefully investigated convergence of the results with respect to inclusion of electron correlation effects and with respect to basis set extent. Theoretical excitation energies obtained from IHFSCC and a subset of GASCI calculations are compiled in table 3 along with theoretical and experimental results from Barker *et al* [29]. All data was calculated at $R = 1.981 \text{ \AA}$ which corresponds to the calculated CCSDT(Q) equilibrium geometry [29] of the $^1\Sigma_0^+$ state. Starting with the GASCI results a clear trend emerges which—nearly independent of the choice of active space composition and/or choice of Hamiltonian—places the $\Omega = 1$ state below the $\Omega = 0^+$ state by about $600\text{--}850 \text{ cm}^{-1}$. This finding seems to be in contradiction to the experimental data by Barker *et al* [29] whereas for the remaining $\Omega = 2, 3$ components, which primarily derive from the $^3\Delta$ state by first-order spin–orbit coupling (SOC), a good

Table 2. CI wavefunction models using refined active spinor spaces; the size of the P_m active space is given, in the name of the models, by an upper index X , which is the number of Kramers pairs in the active space. The model $III^{CI,3}$ thus comprises the minimal active space to describe the $\Omega = 0$ et $\Omega = 1$ states corresponding to $^1\Sigma_0$ and $^3\Delta_1$ in the $A-S$ coupling picture. Models $III^{CI,3}$ and $III^{CI+T,3}$ differ by the highest excitation rank allowed from the hole spaces to the particle space. In the latter, triple excitations are included.

Model	Th 6s,6p F 2s,2p	Th 7s,6d δ	Th 6d π	Th 6d σ	Th 7p π	Th 7p $\sigma,8s$	Below 10 a.u.
$III^{CI,3}$	Q – SD	P_m	Q – SD	Q – SD	Q – SD	Q – SD	Q – SD
$III^{CI+T,3}$	Q – SD	P_m	Q – SDT	Q – SDT	Q – SDT	Q – SDT	Q – SDT
$III^{CI,5}$	Q – SD	P_m	P_m	Q – SD	Q – SD	Q – SD	Q – SD
$III^{CI,6}$	Q – SD	P_m	P_m	P_m	Q – SD	Q – SD	Q – SD
$III^{CI,8}$	Q – SD	P_m	P_m	P_m	P_m	Q – SD	Q – SD
$III^{CI,10}$	Q – SD	P_m	P_m	P_m	P_m	P_m	Q – SD
IV^{CI}	frozen	P_m	P_m	P_m	P_m	P_m	Q – SD

Table 3. Electronic spectra obtained with IHFSCC and MRCI for different model spaces at $R = 1.981$ Å. Unless otherwise noted, results are for TZ basis sets and include the spin-same orbit (SSO) and spin-other orbit interaction (SOO) in an atomic mean-field fashion. Subscripts on the electronic state labels indicate the value of Ω . All energies are given in cm^{-1} . Our best estimate is displayed in boldface.

Method	Model ^{a,f}	Hamiltonian	Electronic state energy				
			$^1\Sigma_{0^+}$	$^3\Delta_1$	$^3\Delta_2$	$^3\Delta_3$	$^3\Pi_{0^-}$
IHFSCC	I^{CC}	2c	285.29	0.00	1063.29	3096.14	5228.76
	II^{CC}	2c	27.89	0.00	1070.40	3166.36	4690.68
	$III^{CC,d}$	2c	42.16	0.00	1062.01	3146.00	4499.13
	$III^{CC,d}$	2c	15.25	0.00	1062.22	3149.47	4510.50
	$III^{CC,e}$	2c	190.85	0.00	1048.27	3156.71	4123.14
	$III^{CC,a}$	2c	0.00	108.26	1157.05	3235.93	4415.96
MRCI	$III^{CC,f}$	2c	318.99	0.00	1038.94	3161.99	3841.17
	I^{CI}	2c	854.32	0.00	1154.40	3188.81	3387.74
	II^{CI}	2c	630.04	0.00	1166.86	2986.27	-
CCSD(T)+SO ^b			500.7	0.0	889.5	2156.8	
CCSDT+SO ^b			143.3	0.0	889.7	2157.1	
CCSDT(Q)+SO ^b			0.0	65.5	955.3	2222.9	
MRCI+Q/SO ^c			0.0	202	1047	2163	
Experiment ^b			0.00	315.0(5)	1052.5(5)	3150(15)	3395(15)

^a 2c-mmF approach and modified QZ basis set for Th ((37s34p26d23f5g1h)).

^b Reference [29].

^c Reference [31].

^d 2c-mmF approach.

^e 2c-mmF approach (QZ basis set, (37s34p26d23f9g5h1i)).

^f 2c-mmF approach and extrapolation to the basis set limit.

agreement is obtained. We also note that accounting in the GASCI expansion for correlation (SD) rather than mere polarization effects (S) from the 5d shell of Th decreases the gap between $\Omega = 0^+$ and $\Omega = 1$ states by approximately 30%.

Turning to the IHFSCC results, the smallest active space calculation (I^{CC}) yields the same picture as was obtained from the MRCI data: the $\Omega = 1$ state is predicted to be the ground state, although the energy gap to the $\Omega = 0^+$ state now reduces to only 285 cm^{-1} . In accord with the observed qualitative trend in the GASCI results, the inclusion of the Th 5d spinors in the correlation space (model II^{CC}) leads to a strong stabilization of the $\Omega = 0^+$ state by $\approx 260 \text{ cm}^{-1}$ with respect to the $\Omega = 1$ state. Interestingly, differential correlation effects of the Th 5d shell hardly affect the relative energy separation between the remaining spin-orbit split states $\Omega = 2, 3$ of the $^3\Delta$ term while the vertical excitation energy from the ground state to the $\Omega = 0^-$ component of the $^3\Pi$ state is lowered by $\approx 10\%$. Next, changing the treatment of the two-electron SSO and SOO corrections to a molecular mean-field approach enlarges the energetic gap between the $\Omega = 1$ and the $\Omega = 0^+$ states to 42 cm^{-1} , a small but perhaps non-negligible effect given the close proximity of the two states. Therefore, all further IHFSCC data have been obtained from 2c-calculations based on the mmf approach.

Using an extended Q correlation space (model $III^{CC,\dagger}$) underlines the above-encountered stabilization of the $\Omega = 0^+$ state compared to the $\Omega = 1$ ground state with respect to the inclusion of core-valence correlations. The additional 4f5s5p correlation brings both states closer by about 30 cm^{-1} which amounts to roughly 10% of

the effect of solely correlating the 5d shell. All remaining Ω states under consideration essentially retain their relative energetic separation. Going from a TZ to a QZ basis set description largely counteracts the correlation trends found above, as the $\Omega = 0^+$ state is now $\approx 190 \text{ cm}^{-1}$ above the $\Omega = 1$ state. To emphasize that this change is primarily a result of the quality of the correlating basis can be seen from table 3 by comparing the original QZ results ($III^{CC,\ddagger}$) to those for the modified QZ basis ($III^{CC,S}$). In the latter case we employ the same QZ spdf function set whereas the higher angular momentum correlation functions resemble the extent of the TZ composition (5g1h). Using this combination places the $\Omega = 0^+$ state below the $\Omega = 1$ state by $\approx 100 \text{ cm}^{-1}$. It becomes apparent that basis set and electron correlation effects strongly influence the relative energetic separation between the $^1\Sigma$ and the $^3\Delta$ terms, but hardly affect the splitting of the Ω components of the $^3\Delta$ term. This is due to differential correlation effects arising from the presence of a Fermi hole in a triplet term and the absence of a Fermi hole in a singlet term, making the latter more sensitive to the description of interelectronic correlations than the former. These, in turn, depend on the quality of the one-particle basis set.

Due to the apparent sensitivity of the system's electronic excitation energies to the quality of the basis set, we performed an extrapolation to the complete basis set limit (model $III^{CC,*}$ in table 3) based on the $III^{CC,\ddagger}$ and $III^{CC,\ddagger}$ data, respectively, according to the expression [57]

$$E[(0h, 2p)]_{\Omega}^{\infty} = \frac{3^3 E[(0h, 2p)]_{\Omega}^{TZ} - 4^3 E[(0h, 2p)]_{\Omega}^{QZ}}{3^3 - 4^3}, \quad (5)$$

where $E[(0h, 2p)]_{\Omega}^X$ ($X = \text{TZ, QZ}$) denotes the absolute energy in the sector (0h, 2p) of each of the states under consideration. The extrapolated relative term energies are roughly within 10 cm^{-1} of the experimental ones for the $^1\Sigma_0^+$ and the components of the $^3\Delta$ state, if one assumes an inversion of the experimental assignment for the two lowest electronic states. For the $^3\Pi_0^-$ state the discrepancy with experiment is considerably larger (about 440 cm^{-1}).

The results of Barker *et al* [29]—based on spin-free open-shell coupled-cluster (CC) up to perturbative quadruples (CCSDT(Q)) combined *a posteriori* with SOC parameters obtained from a spin-orbit multireference configuration interaction (MRCI) calculation—show that cluster excitation ranks higher than Doubles play an important role in determining the relative energies of $^1\Sigma_0^+$ and $^3\Delta^1$, which is not surprising as this is a showcase for differential correlation effects (for the above-mentioned reasons). The IHFSCC models do not contain Triples and Quadruples excitations in the projection manifold, and so a downward correction on the $^1\Sigma_0^+$ energy from model $III^{CC,*}$ is to be expected. On the other hand, all models of Barker *et al*, including the MRCI+Q/SO result from [31], yield a $^3\Delta_1$ – $^3\Delta_2$ separation of roughly 900 cm^{-1} , whereas the experimental splitting is 740 cm^{-1} (or 1050 cm^{-1} assuming an inverted assignment). Even poorer is the $^3\Delta_2$ – $^3\Delta_3$ splitting for the model CCSDT(Q)+SO of 1270 cm^{-1} compared with the experimental splitting of about 2100 cm^{-1} . Such a large error suggests that the perturbative treatment of spin-orbit interaction in a framework of Λ – S -coupled states is questionable for the respective state manifold of ThF^+ . For instance, a larger splitting of the $^3\Delta$ components would shift the $^3\Delta_1$ state to an energy lower than that of $^1\Sigma_0^+$ in the perturbative CC calculations of Barker *et al*.

In contrast to this, the $^3\Delta_2$ – $^3\Delta_3$ splitting from the rigorous non-perturbative CC model $III^{CC,*}$ of 2120 cm^{-1} is in excellent agreement with the experimental value of 2100 cm^{-1} . The rigorous non-perturbative CI models yield similar results. Therefore, the remaining uncertainty in the calculations of Barker *et al* seem to be greater than those in the present calculations. Although their electron correlation treatment is of higher order than ours, it is obvious that our non-perturbative treatment of SOC is essential in obtaining the correct ground state.

In order to shed further light on the relative energies of the $^1\Sigma_0^+$ and $^3\Delta_1$ states and to verify whether these states may cross in the vicinity of their respective minima we calculated spectroscopic constants for both states from a quartic polynomial fit (program `twofit` provided by DIRAC) for a series of five equally-spaced ($\pm 0.025 \text{ \AA}$ and $\pm 0.050 \text{ \AA}$) data points around 1.981 \AA using the computational model $III^{CC,*}$. The resulting minimum internuclear distances (R_e), harmonic frequencies (ω_e) and anharmonicity constants ($\omega_e x_e$) are compiled in table 4 together with the data of Barker *et al* [29].

Considering the equilibrium internuclear distance R_e our IHFSCC as well as the other theoretical results are close enough to be consistent with the average value of $R_0 = 1.98(2) \text{ \AA}$ determined from the measurements of the rotational constants B_0 [29]. We further note that our calculated harmonic vibrational frequencies are similar to the CCSDT(T)+SO results, in particular for the $\Omega = 0^+$ state, but overestimate both the experimental values and the theoretical benchmark CCSDT(Q)+SO of Barker *et al* by about 10 – 14 cm^{-1} . Although not very large, the discrepancy is not unexpected, since this property is in general sensitive to the extent to which dynamic electron correlations are accounted for.

Assuming a correct experimental assignment, we find rather large discrepancies for the anharmonicity constants, deviating by about 0.3 cm^{-1} for the $^1\Sigma_0^+$ and -1 cm^{-1} for the $^3\Delta_1$ state. Reversing the experimental assignment would improve the picture and reduce the discrepancies to -0.2 cm^{-1} and -0.6 cm^{-1} for the two

Table 4. Spectroscopic constants for the lowest two electronic states of ThF⁺ in comparison with other theoretical and experimental work by Barker *et al* [29].

State		ω_e/cm^{-1}	$\omega_e x_e/\text{cm}^{-1}$	R_e (Å)
$^3\Delta_1$	CCSDT(Q) + SO ^a	651.1		1.993
	CCSD(T) + SO ^a	654.1		1.992
	IHFSCC <i>III</i> ^{CC,*}	667.3	1.268	1.984
	Experiment ^a	658.3(10)	2.3(5)	
$^1\Sigma_0^+$	CCSDT(Q) + SO ^a	659.8		1.981
	CCSD(T) + SO ^a	672.3		1.975
	CCSD(T) ^b	675.7		1.973
	IHFSCC <i>III</i> ^{CC,*}	670.8	2.088	1.974
	Experiment ^a	656.8(10)	1.85(25)	

^a Reference [29].^b Reference [59]; calculations on the $^1\Sigma_0^+$ state are assumed.**Table 5.** Vertical excitation energy for $\Omega = 0^+$, electron EDM effective electric field, magnetic hyperfine interaction constant, and scalar–pseudoscalar electron–nucleon interaction constant for $\Omega = 1$ at an internuclear distance of $R = 3.779 a_0$ using basis sets with increasing cardinal number and the wavefunction model *III*^{CT,5}.

Basis set	$T_v(\text{cm}^{-1})$	$E_{\text{eff}}(\text{GV cm}^{-1})$	$A_{\parallel}(\text{MHz})$	$W_{P,T}$ (kHz)
DZ	378	37.8	1824	51.90
TZ'	787	36.9	1836	50.73
QZ'	877	36.9	1830	50.77

states, respectively. However, this average discrepancy is still about as large as the difference between the experimental anharmonicity constants for the two states in question. We, therefore, regard this finding as an indication but not as conclusive.

Based on the calculated spectroscopic constants, the potential minima of the discussed Ω states spread over a range of only 0.01 Å and are also very close to the reference value used for the calculations presented in table 3. This in turn means that the corresponding vertical excitation energies have to be close to the adiabatic ones. Based on the FSCC energies extrapolated to the basis-set limit, we estimate an adiabatic separation of 313.6 cm⁻¹ between the $\Omega = 1$ and $\Omega = 0^+$ states, or 317 cm⁻¹ for the 0–0 transition between the vibrational ground states.

3.2.2. \mathcal{P} , \mathcal{T} -odd and magnetic hyperfine interaction constants

We now turn to the discussion of our results of direct relevance to the search for \mathcal{P} , \mathcal{T} -odd effects in ThF⁺. We have used a series of one-particle basis sets and CI models, all of which are defined in subsection 3.1 and table 2.

In order to minimize error bars we test the influence of several criteria, the first of which is the quality of the basis set. The results in table 5 demonstrate that the effective electric field and the parallel magnetic hyperfine interaction constant (for ²²⁹Th ($I = 5/2$)) are rather insensitive to the size of the basis set employed. Increasing the basis set cardinal number changes the value of the hyperfine interaction constant A_{\parallel} by less than 0.6% in magnitude. Likewise, the correction yielded by the TZ' basis set for the effective electric field E_{eff} is smaller than 2% and the use of the QZ' basis set leads to a further change of less than 0.1%. The latter very small correction is also found for the electron–nucleon interaction constant. The vertical excitation energy for $\Omega = 0$ (T_v) undergoes a slightly larger change. Replacing the DZ by the TZ' basis set doubles the value of T_v , an increase of 409 cm⁻¹ on the absolute. Using the set of QZ' quality yields a correction of 11% in magnitude, less than 90 cm⁻¹. The sensitivity of this excitation energy to basis set extent was already observed in the results in table 3. However, based on the results in table 5 we conclude that the values of E_{eff} , A_{\parallel} and $W_{P,T}$ for $\Omega = 1$ are sufficiently converged with the TZ' basis set, allowing us to use this basis set for further analysis.

The results in table 6 show that wavefunctions accounting only for correlation effects among the two outermost valence electrons (\mathcal{IV}^{CT}) are too approximate for determining E_{eff} , A_{\parallel} and $W_{P,T}$ for $\Omega = 1$, although they do yield a correct qualitative description of the low-lying electronic valence states of the molecule and, in some cases, benefit from favorable error cancellations. It has been shown in [14] on the isoelectronic ThO molecule that these properties are essentially unaffected by accounting for electron correlations arising from Th core shells, and the reason for this has been explained via orbital (more precisely, spinor) perturbation theory.

Table 6. Vertical excitation energy for $\Omega = 0^+$, electron EDM effective electric field, magnetic hyperfine interaction constant, and scalar–pseudoscalar electron–nucleon interaction constant for $\Omega = 1$ at an internuclear distance of $R = 3.779 a_0$ using the TZ' basis set, varying number of correlated electrons and varying active spinor spaces.

CI model (TZ basis)	T_v (cm ⁻¹)	E_{eff} (GV cm ⁻¹)	A_{\parallel} (MHz)	$W_{p,T}$ (kHz)
IV^{CI}	274	35.4	1749	49.44
$III^{CI,3}$	1029	47.5	1842	65.78
$III^{CI,5}$	787	36.9	1836	50.73
$III^{CI,6}$	709	36.2	1836	49.90
$III^{CI,8}$	598	35.6	1834	49.04
$III^{CI,10}$	538	35.2	1833	48.35

Table 7. Vertical excitation energy for $\Omega = 0^+$, electron EDM effective electric field, magnetic hyperfine interaction constant, and scalar–pseudoscalar electron–nucleon interaction constant for $\Omega = 1$ at an internuclear distance of $R = 3.779 a_0$ using the DZ basis set and varying maximum excitation rank.

CI model (DZ basis)	T_v (cm ⁻¹)	E_{eff} (GV cm ⁻¹)	A_{\parallel} (MHz)	$W_{p,T}$ (kHz)
$III^{CI,3}$	654	47.0	1830	64.92
$III^{CI,10}$	88	37.1	1832	51.06
$III^{CI+T,3}$	247	35.4	1834	48.64

We have therefore carried out a study of the influence of the active spinor space, models of type $III^{CI,X}$, and restricting the electron correlation treatment to the outermost electronic shells (Th 6s, 6p, 7s, 6d, F 2s, 2p).

Our findings are very similar to those obtained for ThO in [14]. Increasing the size of the active space leads to significant corrections to the vertical excitation energy. The greatest change occurs when adding the energetically following π -type spinors to the minimal active space (step from $X = 3$ to $X = 5$). A similar drop of the values of the effective electric field and the hyperfine interaction constant is here observed. Including the energetically following spinors entails further decrease of all studied properties, but significantly less pronounced than the previous ones.

In view of the significant changes of the results when increasing the active spinor space, one could ponder the necessity to include excitation ranks higher than Doubles into the set of virtual spinors. We investigated this using the DZ basis (due to computational cost), and the results can be found in table 7. The hyperfine interaction constant A_{\parallel} is insensitive to these higher excitations, allowing triple excitations to the virtual space changes the value by only 0.2%. However, the effective electric field as well as the S–PS interaction constant exhibit a strong dependence on higher excitations. The inclusion of triple excitations yields a drop of 25% in magnitude, respectively. Interestingly, this dramatic decrease is also observed when excluding triple excitations and augmenting the active spinor space by seven additional σ - and π -type Kramers pairs. Such an augmentation introduces a subset of triple and a subset of quadruple excitations but avoids terms with three or more particles in the external spinor space, therefore leading to a much shorter CI expansion. The additional excitation classes can be written symbolically as (core)^{*h*}, (active)^{*p*}, (external)^{*q*}, where ‘active’ denotes the *additional* active-space spinors, *h* denotes the number of holes and *p* and *q* the number of particles in the respective spinor space. In case of the triples, the additional sets of configurations then read as (*h* = 1, *p* = 3, *q* = 0), (*h* = 1, *p* = 2, *q* = 1) and (*h* = 2, *p* = 1, *q* = 2). For the quadruples one obtains only (*h* = 2, *p* = 2, *q* = 2). Evidently, the augmentation of the active space largely covers the set of Triple excitations that are required for obtaining accurate values of E_{eff} , A_{\parallel} , and $W_{p,T}$. In case of the excitation energies we observe that the additional Quadruple excitations, which are not present in the model $III^{CI+T,3}$, have a significant effect of stabilizing the Σ state relative to the Δ state, in accord with the discussion in the previous section.

In order to gain insight into the character of the excitations leading to important corrections, we carried out a detailed analysis of the wavefunction expansions referred to as $III^{CI,3}$ and $III^{CI,5}$. They turn out to be very similar, the expansion coefficients remaining almost unchanged with the exception of a determinant that is the next-to-leading contributor with a coefficient $c \approx 0.046$ in the expansion of $III^{CI,5}$ whereas its coefficient is much smaller in the $III^{CI,3}$ expansion ($c < 0.01$). This respective determinant can be written as a $\delta_{6d}^1(\pi\sigma)^1$ occupation which corresponds to a single excitation with respect to the leading determinant $\sigma_7^1\delta_{6d}^1$ for this $\Omega = 1$ state. Since $\delta_{6d}^1(\pi\sigma)^1$ is already contained in the $III^{CI,3}$ expansion, it is necessarily the additional higher excitations included in the $III^{CI,5}$ expansion which lend amplitude to the $\delta_{6d}^1(\pi\sigma)^1$ determinant.

We carried out a Mulliken population analysis of the spinors occupied in this decisive determinant. $\pi\sigma$ denotes a spinor of π -character with significant admixture of σ -character (see the fourth spinor in table 8). In

Table 8. Characterization of active-space Kramers pairs in the TZ' basis. Orbital angular momentum projection, spinor energy and principal atomic shell character.

Spinor(λ)	$\langle \hat{I}_z \rangle_{\varphi_i}$	$\varepsilon_{\varphi_i} [E_H]$	atomic character
σ	-0.001	-0.43	85% Th(s)
δ	1.966	-0.42	98% Th(d)
δ	-2.000	-0.41	99% Th(d)
$\pi\sigma$	-0.720	-0.14	50% Th(p), 45% Th(d)
π	1.025	-0.13	60% Th(d), 36% Th(p)
$\sigma\pi$	-0.290	-0.12	47% Th(d), 43% Th(p)
π	-0.980	-0.10	55% Th(p), 36% Th(d)
π	1.011	-0.09	64% Th(p), 29% Th(d)
σ	-0.005	-0.07	59% Th(p), 19% Th(f), 15% Th(d)
σ	-0.014	-0.06	90% Th(s)
$\pi\sigma$	-0.894	-0.03	89% Th(p)
π	1.006	-0.03	94% Th(p)
σ	-0.097	-0.02	65% Th(p), 29% Th(f)

this case, the spinor is of Th(p) character with a 45% contribution of Th(d). Hence, the drop of the values of E_{eff} , A_{\parallel} and $W_{P,T}$ is related to a shift of electron density from Th(7s) to Th(p) and Th(d), the two latter of which have an approximate angular node at the nucleus. It is, therefore, physically plausible that the mentioned higher excitations which lead to a shift of electron (spin) density from Th(s) to higher angular momentum entail a reduction of the EDM effective electric field and of the magnetic hyperfine interaction constant.

3.2.3. EDMs and transition dipole moments

The electron EDM effective field stands in direct relationship with the static molecular electric dipole moment. We calculated this latter quantity as an expectation value over relativistic CI wavefunctions, and in addition, electric dipole transition moments between different electronic states in an energy window of up to roughly 8000 cm^{-1} . The results are compiled in tables 9 and 10. Concerning the notation for electronic states we have here added information on dominant and minor contributors in Λ -S coupling to a given well-defined Ω state.

The absolute molecular dipole moment is very large for ThF^+ , especially for the low-lying electronic states, and reaches into the range of the largest dipole moments for diatomic molecules. Concerning transition dipole moments we observe a generally good agreement with expected selection rules for transitions between different $2S+1\Lambda_{\Omega}$ states. For example, the largest matrix element, $|\langle {}^3\Phi_2({}^3\Pi_2) | \hat{D} | {}^3\Delta_1 \rangle| = 1.34 \text{ [D]}$, is spin-allowed ($\Delta S = 0$) and also orbital angular momentum allowed (here $\Delta\Lambda = \pm 1$). In addition, $\Delta\Omega = \pm 1$ is also satisfied. On the other hand, very small transition moments are typically found for spin-forbidden transitions. Our study of transition moments covers a few more states than those reported in a recent study on actinide bonding by Heaven *et al* [31], and the results agree quite well with the values obtained in that reference.

The comparison of tables 9 and 10 shows that our larger set of results obtained with the smaller two-electron CI expansion agrees quite well with the results from the more elaborate CI model, II^{CI} . We therefore consider the values in table 9 as a good approximation to the accurate values.

4. Conclusion

In the earlier work of Barker *et al* [29, 31] $\Omega = 0^+$ had been proposed as the electronic ground state of ThF^+ , supported by the measured intensities of the lowest band compared to those of other bands in a pulsed field ionization — zero kinetic energy experiment. Accompanying many-body electronic structure calculations were judged to be inconclusive in this regard. From our detailed discussion of relativistic many-body calculations, including those from [29] for excitation energies, we conclude that the assignment of the ground electronic state of ThF^+ remains an open issue. The models of Barker *et al* suffer from the incomplete account of spin-orbit interaction and its intertwining with dynamic electron correlations, which becomes manifest in the poor description of the energetic splitting of the ${}^3\Delta$ state into its Ω components. Our present study takes these effects into account rigorously which leads to a ${}^3\Delta_1$ ground state. Our models lack excitation ranks with three or more external particles in the wave operator, the inclusion of which may have the effect of inverting the energetic order of ${}^3\Delta_1$ and ${}^1\Sigma_0^+$ due to considerable differential correlation effects. On the other hand, the model spaces we have used in the IHFSCC calculations do give rise to a subset of excitation ranks higher than doubles in the projection manifold, which should mitigate the uncertainty in our best present calculation (boldface in table 3). Giving preference to assigning the ground state as ${}^1\Sigma_0^+$ is, therefore, no longer tenable from a theoretical point of view,

Table 9. Molecular static electric dipole moments $\langle {}^M A_{\Omega} | \hat{D}_z | {}^M A_{\Omega} \rangle$, transition dipole moments $|\langle {}^M A'_{\Omega} | \hat{D} | {}^M A_{\Omega} \rangle|$, with \hat{D} the electric dipole moment operator (both in [D] units), and vertical transition energies for low-lying electronic states using the TZ' basis set and the CI model \mathcal{TV}^{CT} . The origin is at the center of mass, and the internuclear distance is $R = 3.779 a_0$. (${}^M A_{\Omega}$) denotes a term contributing at least 10% to the state. 1,3 denotes cases where Λ -S coupling breaks down significantly according to the analysis of our spinor-based ω - ω coupled wavefunctions.

${}^M A_{\Omega}$ state	T_v (cm $^{-1}$)	${}^1\Sigma_0^+$	${}^3\Delta_1$	${}^3\Delta_2$	${}^3\Delta_3$	${}^1\Sigma_0$ (${}^3\Pi_0$)	${}^3\Pi_0$	${}^{1,3}\Pi_1$ (${}^3\Sigma_1$)	${}^3\Pi_0$ (${}^1\Sigma_0$)	${}^{1,3}\Delta_2$ (${}^3\Pi_2$)	${}^3\Sigma_1$	${}^{1,3}\Pi_1$	${}^3\Phi_2$ (${}^3\Pi_2$)
${}^1\Sigma_0^+$	274	-4.004											
${}^3\Delta_1$	0	0.012	-4.075										
${}^3\Delta_2$	724	0.000	0.070	-4.022									
${}^3\Delta_3$	2198	0.000	0.000	0.052	-4.075								
${}^1\Sigma_0$ (${}^3\Pi_0$)	6344	0.439	0.455	0.000	0.000	-3.752							
${}^3\Pi_0$	6528	0.000	0.571	0.000	0.000	0.000	-2.116						
${}^{1,3}\Pi_1$ (${}^3\Sigma_1$)	6639	0.868	0.142	0.218	0.000	0.197	0.000	-2.375					
${}^3\Pi_0$ (${}^1\Sigma_0$)	6747	0.003	0.391	0.000	0.000	0.929	0.000	0.094	-2.717				
${}^{1,3}\Delta_2$ (${}^3\Pi_2$)	7008	0.000	0.473	0.334	0.298	0.000	0.000	0.529	0.000	-2.734			
${}^3\Sigma_1$	7490	0.226	0.069	0.221	0.000	0.136	0.197	0.451	0.145	0.087	-4.463		
${}^{1,3}\Pi_1$	7918	0.667	0.052	0.801	0.000	0.011	0.064	0.107	0.043	0.444	0.209	-2.708	
${}^3\Phi_2$ (${}^3\Pi_2$)	8245	0.000	1.338	0.234	0.272	0.000	0.000	0.134	0.000	0.384	0.018	0.099	-2.271

Table 10. Molecular static electric dipole moments $\langle {}^M\Lambda_{\Omega} | \hat{D}_z | {}^M\Lambda_{\Omega} \rangle$, with \hat{D} the electric dipole moment operator, using the TZ basis set and the CI model III^{CT} . The origin is at the center of mass, and the internuclear distance is $R = 3.779 a_0$ (F nucleus at $z\hat{e}_z$ with $z < 0$). ${}^M\Lambda$ is an approximate notation and refers to the term derived from the leading Slater determinants and the information in table 8.

${}^M\Lambda_{\Omega}$ State	T_v (cm ⁻¹)	$\langle {}^M\Lambda_{\Omega} \hat{D}_z {}^M\Lambda_{\Omega} \rangle$ (D)
${}^1\Sigma_0^+$	630	3.941
${}^3\Delta_1$	0	4.029
${}^3\Delta_2$	1167	3.970
${}^3\Delta_3$	2986	4.034

Table 11. Effective electric field for the science states of selected diatomic candidate molecules in search of parity- and time-reversal violation.

Molecule	Electronic state	E_{eff} (GV cm ⁻¹)
ThO	${}^3\Delta_1$	75.2 ^a , 81.5 ^b
YbF	${}^2\Sigma_{1/2}^+$	26 ^c , 25 ^d , 24 ^e
PbO	${}^3\Sigma_1^+$	25 ^f
ThF ⁺	${}^3\Delta_1$	35.2 ^g , 90 ^h
WC	${}^3\Delta_1$	-36 ⁱ

^a Reference [14].

^b Reference [60].

^c Reference [61].

^d Reference [62].

^e Reference [63].

^f Reference [64].

^g This work.

^h Reference [24].

ⁱ Reference [20].

based on our present findings. In any case, it is beyond reasonable doubt that the two respective states are the lowest-lying electronic states and that they are so close in energy that an eEDM experiment could be carried out irrespective of their ordering [32].

We conclude that our best model for the determination of \mathcal{P} , \mathcal{T} -odd and magnetic hyperfine interaction constants is $III^{CT,10}$ in the TZ' basis set (boldface in table 6), which displays property values nearly converged with respect to the different degrees of freedom in the models we have tested. Our best prediction for the hyperfine constant in the $\Omega = 1$ 'science state' is 1833 MHz, which awaits confirmation from an experimental measurement. The obtained effective electric field of $E_{\text{eff}} = 35.2$ GV cm⁻¹ in this same state is more than 60% smaller than the value of $E_{\text{eff}} = 90$ GV cm⁻¹ obtained earlier by Meyer *et al* [24]. The large deviation is very likely to be due to the limited set of electronic configurations and further model-inherent approximations used in the approach of Meyer *et al*. The smaller value of E_{eff} is a setback for potential electron EDM searches with this molecular ion, but given the body of other favorable properties (low-lying ${}^3\Delta_1$ state, large molecular dipole moment) of ThF⁺ still large enough to retain the system as a promising candidate in search of \mathcal{P} , \mathcal{T} violation. In table 11 we provide a summary of E_{eff} values in the respective science states of some diatomic molecules of current interest in this search. Our E_{eff} presently determined for ThF⁺ is still larger than E_{eff} in the science state of the YbF molecule, in which a new upper bound to the electron EDM had been determined in 2011 [58]. The static electric transition dipole moments we have determined for a set of states below 9000 cm⁻¹ in ThF⁺ may also be helpful in devising a route for state preparation for an EDM measurement in this promising molecular ion.

Acknowledgments

MD, MKN, and TF thank the *Agence Nationale de la Recherche* (ANR) through grant no. ANR-BS04-13-0010-01, project 'EDMeDM', for financial support. This work was granted access to the HPC resources of CALMIP under the allocation 2014-p1424. ASPG acknowledges support from PhLAM (Unité Mixte de Recherche de l'Université de Lille 1 et du CNRS), the French National Research Agency (Contract ANR-11-LABX-0005 'Chemical and Physical Properties of the Atmosphere' (CaPPA)), and the European Commission through the FP7 TALISMAN project (Contract No. 323300). We are grateful for HPC resources from GENCI-CCRT (Grant 2013-081859) and the Danish Center for Scientific Computing (DCSC) at SDU Odense. We thank Eric Cornell (JILA, Boulder) for helpful comments and Radovan Bast (Stockholm) for technical support.

References

- [1] Dine M and Kusenko A 2004 Leptonic CP violation *Rev. Mod. Phys.* **76** 1
- [2] Sakharov A D 1967 Violation of CP invariance, C asymmetry, and baryon asymmetry of the Universe *JETP Lett.* **5** 24
- [3] Pospelov M and Ritz A 2005 Electric dipole moments as probes of new physics *Ann. Phys.* **318** 119
- [4] Fortson N, Sandars P and Barr S 2003 *Phys. Today* **56** 33–39
- [5] Streater R F and Wightman A S 1964 *PCT, Spin and Statistics, and All That* (New York: W A Benjamin)
- [6] Sachs R G 1987 *The Physics of Time Reversal* (Chicago, IL: University of Chicago Press)
- [7] Roberts B L and Marciano W J 2009 The electric dipole moment of the electron *Lepton Dipole Moments (Advances Series on Directions in High Energy Physics vol 20)* ed E D Commins and D DeMille (New Jersey: World Scientific) chapter 14, pp 519–81
- [8] Liu Z W and Kelly H P 1992 Analysis of atomic electric dipole moment in thallium by all-order calculations in many-body perturbation theory *Phys. Rev. A* **45** R4210
- [9] Bernreuther W and Suzuki M 1991 The electric dipole moment of the electron *Rev. Mod. Phys.* **63** 313
- [10] Sushkov O P and Flambaum V V 1978 Parity breaking effects in diatomic molecules *Sov. Phys.—JETP* **48** 608
- [11] Sandars P G H 1965 The electric dipole moment of an atom *Phys. Lett.* **14** 194
- [12] Regan B C, Commins E D, Schmidt C J and DeMille D 2002 New limit on the electron electric dipole moment *Phys. Rev. Lett.* **88** 071805
- [13] Baron J et al The ACME Collaboration 2014 Order of magnitude smaller limit on the electric dipole moment of the electron *Science* **343** 269
- [14] Fleig T and Nayak M K 2014 Electron electric dipole moment and hyperfine interaction constants for ThO *J. Mol. Spectrosc.* **300** 16
- [15] Skripnikov L V, Petrov A N and Titov A V 2013 Communication: theoretical study of ThO for the electron electric dipole moment search *J. Chem. Phys.* **139** 221103
- [16] DeMille D and On behalf of the ACME collaboration 2014 ASME: search for the electron's electric dipole moment *24th Int. Conf. on Atomic Physics (ICAP 2014), (Washington, DC, 3-8 August 2014)* (<http://icap2014.org/book-abstracts-download>)
- [17] Leanhardt A E, Bohn J L, Loh H, Maletinsky P, Meyer E R, Sinclair L C, Stutz R P and Cornell E A 2011 High-resolution spectroscopy on trapped molecular ions in rotating electric fields: a new approach for measuring the electron electric dipole moment *J. Mol. Spectrosc.* **270** 1
- [18] Cossel K C et al 2012 Broadband velocity modulation spectroscopy of HfF⁺: towards a measurement of the electron electric dipole moment *Chem. Phys. Lett.* **546** 1
- [19] Meyer E R, Bohn J L and Deskevich M P 2006 Candidate molecular ions for an electron electric dipole moment experiment *Phys. Rev. A* **73** 062108
- [20] Lee J, Chen J, Skripnikov L V, Petrov A N, Titov A V, Mosyagin N S and Leanhardt A E 2013 Optical spectroscopy of tungsten carbide for uncertainty analysis in electron electric dipole moment search *Phys. Rev. A* **87** 2013
- [21] Wang F and Steimle T C 2011 Communication: electric dipole moment and hyperfine interaction of tungsten monocarbide, WC *J. Chem. Phys.* **134** 201106
- [22] Petrov A N, Mosyagin N S, Isaev T A and Titov A V 2007 Theoretical study of HfF⁺ in search for the electron electric dipole moment *Phys. Rev. A* **76** 030501
- [23] Fleig T and Nayak M K 2013 Electron electric-dipole-moment interaction constant for HfF⁺ from relativistic correlated all-electron theory *Phys. Rev. A* **88** 032514
- [24] Meyer E R and Bohn J L 2008 Prospects for an electron electric-dipole moment search in metastable ThO and ThF⁺ *Phys. Rev. A* **78** 010502
- [25] Adam A G, Hopkins W S and Tokaryk D W 2004 High-resolution visible laser spectroscopy of HfF *J. Mol. Spectrosc.* **225** 1
- [26] Barker B J, Antonov I O, Bondybey V E and Heaven M C 2011 Communication: spectroscopic measurements for HfF⁺ of relevance to the investigation of fundamental constants *J. Chem. Phys.* **134** 201102
- [27] Petrov A N, Mosyagin N S and Titov A V 2009 Theoretical study of low-lying electronic terms and transition moments for HfF⁺ for the electron electric dipole moment search *Phys. Rev. A* **79** 012505
- [28] Skripnikov L V, Mosyagin N S, Petrov A N and Titov A V 2009 *JETP Lett.* **88** 578
- [29] Barker B J, Antonov I O, Heaven M C and Peterson K A 2012 Spectroscopic investigations of ThF and ThF⁺ *J. Chem. Phys.* **136** 104305
- [30] Irikura K K 2013 *J. Phys. Chem. A* **117** 1276
- [31] Heaven M C, Barker B J and Antonov I O 2014 Spectroscopy and structure of the simplest actinide bonds *J. Phys. Chem. A* **118** 10867
- [32] Cornell E A and Gresh D N 2014 private communication
- [33] Lindroth E, Lynn B W and Sandars P G H 1989 Order α^2 theory of the atomic electric dipole moment due to an electric dipole moment on the electron *J. Phys. B* **22** 559
- [34] Kozlov M G 1985 Semiempirical calculations of *P*- and *P*, *T*-odd effects in diatomic molecules-radicals *Zh. Eksp. Teor. Fiz.* **89** 1933
- [35] Saue T and Visscher L 2003 Four-component electronic structure methods for molecules *Theoretical Chemistry and Physics of Heavy and Super Heavy Elements* ed U Kaldor and S Wilson (Dordrecht: Kluwer)
- [36] Čárský P, Paldus J and Pittner J (ed) 2010 *Recent Progress in Coupled Cluster Methods* (Heidelberg, Germany: Springer)
- [37] Visscher L, Eliav E and Kaldor U 2001 Formulation and implementation of the relativistic Fock-space coupled-cluster method for molecules *J. Chem. Phys.* **115** 9720

- [38] Landau A, Eliav E, Ishikawa Y and Kaldor U 2001 Intermediate Hamiltonian Fock-space coupled cluster method in the one-hole one-particle sector: excitation energies of xenon and radon *J. Chem. Phys.* **115** 6862–5
- [39] Landau A, Eliav E, Ishikawa Y and Kaldor U 2000 Intermediate Hamiltonian Fock-space coupled-cluster method: excitation energies of barium and radium *J. Chem. Phys.* **113** 9905–10
- [40] Landau A, Eliav E and Kaldor U 1999 Intermediate Hamiltonian Fock-space coupled-cluster method *Chem. Phys. Lett.* **313** 399
- [41] Landau A, Eliav E, Ishikawa Y and Kaldor U 2004 Mixed-sector intermediate Hamiltonian Fock-space coupled-cluster approach *J. Chem. Phys.* **121** 6634
- [42] Fleig T, Olsen J and Marian C M 2001 The generalized active space concept for the relativistic treatment of electron correlation: I. Kramers-restricted two-component configuration interaction *J. Chem. Phys.* **114** 4775
- [43] Fleig T, Olsen J and Visscher L 2003 The generalized active space concept for the relativistic treatment of electron correlation: II. Large-scale configuration interaction implementation based on relativistic 2- and 4-spinors and its application *J. Chem. Phys.* **119** 2963
- [44] Knecht S, Aa Jensen H J and Fleig T 2010 Large-scale parallel configuration interaction: II. Two- and four-component double-group general active space implementation with application to BiH *J. Chem. Phys.* **132** 014108
- [45] Jensen H J A et al 2012 DIRAC, a relativistic *ab initio* electronic structure program, Release DIRAC12 www.diracprogram.org
- [46] Bast R et al 2011 DIRAC, a relativistic *ab initio* electronic structure program, Release DIRAC11 <http://dirac.chem.vu.nl>
- [47] Dyall K G 2006 Relativistic double-zeta, triple-zeta, and quadruple-zeta basis sets for the actinides ac-Ir *Theor. Chim. Acta* **90** 491
- [48] Dyall K G 2012 Core correlating basis functions for elements 31–118 *Theor. Chim. Acta* **131** 1217
- [49] Dunning T H Jr 1989 Gaussian basis sets for use in correlated molecular calculations. I. the atoms boron through neon and hydrogen *J. Chem. Phys.* **90** 1007
- [50] Iliáš M and Saue T 2007 An infinite-order two-component relativistic hamiltonian by a simple one-step transformation *J. Chem. Phys.* **126** 064102
- [51] Hess B A, Marian C M, Wahlgren U and Gropen O 1996 A mean-field spin-orbit method applicable to correlated wavefunctions *Chem. Phys. Lett.* **251** 365–71
- [52] Schimmelpfennig B, Maron L, Wahlgren U, Teichteil C, Fagerli H and Gropen O 1998 On the combination of ECP-based CI calculations with all-electron spin-orbit mean-field integrals *Chem. Phys. Lett.* **286** 267
- [53] Sikkema J, Visscher L, Saue T and Iliáš M 2009 The molecular mean-field approach for correlated relativistic calculations *J. Chem. Phys.* **131** 124116
- [54] Eliav E, Borschevsky A, Shamasundar K R, Pal S and Kaldor U 2009 *Int. J. Quantum Chem.* **109** 2909
- [55] Kramida A, Ralchenko Y, Reader J and NIST ASD Team 2013 NIST Atomic Spectra Database (version 5.1) (Gaithersburg, MD.: National Institute of Standards and Technology) (<http://physics.nist.gov/asd>)
- [56] Kazakov G A, Litvinov A N, Romanenko V I, Yatsenko L P, Romanenko A V, Schreitl M, Winkler G and Schumm T 2012 Performance of a ^{229}Th solid-state nuclear clock *New J. Phys.* **14** 083019
- [57] Helgaker T, Jørgensen P and Olsen J 2000 *Molecular Electronic Structure Theory* (Chichester: Wiley)
- [58] Hudson JJ, Kara D M, Smallman I J, Sauer B E, Tarbutt M R and Hinds E A 2011 Improved measurement of the shape of the electron *Nature* **473** 493
- [59] Thanthiriwatte K S, Wang X, Andrews L, Dixon D A, Metzger J, Vent-Schmidt T and Riedel S H 2014 *J. Phys. Chem. A* **118** 2107
- [60] Skripnikov L V and Titov A V 2015 Theoretical study of thorium monoxide for the electron electric dipole moment search: electronic properties of $H^3\Delta_1$ in ThO *J. Chem. Phys.* **142** 024301
- [61] Kozlov M G 1997 Enhancement of the electric dipole moment of the electron in the YbF molecule *J. Phys. B* **30** L607
- [62] Mosyagin N S, Kozlov M G and Titov A V 1998 *J. Phys. B* **31** L763
- [63] Parpia F 1998 *Ab initio* calculation of the enhancement of the electric dipole moment of an electron in the YbF molecule *J. Phys. B* **31** 1409
- [64] Kozlov M G and DeMille D 2002 Enhancement of the electric dipole moment of the electron in PbO *Phys. Rev. Lett.* **89** 133001